

activation energies of 1–11 kcal/mol and widely separated speeds. The RRD theory qualitatively explains these DDLS spectral results. In terms of the theory, the orientational correlation function measured in DDLS spectra of CPM/PMMA samples initially decays at a rapid rate characteristic of neat CPM, indicating a restricting cone angle of about 25–60°. The RRD theory predicts from the intensity and rate of this initial decay a “true” or transformed rotational diffusion coefficient that is not very different from that of neat CPM (and approaches it at high concentrations and temperatures). After the rapid initial decay, the orientational correlation function then decays over a wide range of time scales that apparently reflect the slower relaxation rates of the restricting surroundings. The simple RRD theory used here does not quantitatively treat coupling between the rods and their restricting environment so that it cannot predict the form of the orientational correlation function over the entire relaxation range. Extensions of the RRD theory to include these couplings would be very useful in interpreting the slower relaxation times observed in these experiments.

**Acknowledgment.** This work was supported by National Science Foundation Grant No. CHE 82-00512, the IBM Corp., and the NSF-MRL program through the Center for Materials Research at Stanford University.

**Registry No.** CPM, 831-81-2; PMMA, 9011-14-7.

## References and Notes

- (1) Higashigaki, Y.; Wang, C. H. *J. Chem. Phys.* 1981, 74, 3175.
- (2) Patterson, G. D. *Annu. Rev. Mater. Sci.* 1983, 13, 219.
- (3) Dorfmueller, T., et al. *J. Chem. Phys.* 1979, 71, 366.
- (4) Ouano, A. C.; Pecora, R. *Macromolecules* 1980, 13, 1167, 1173.
- (5) Berne, B. J.; Pecora, R. “Dynamic Light Scattering”; Wiley: New York, 1976.
- (6) Wang, C.-C.; Pecora, R. *J. Chem. Phys.* 1980, 72, 5333.
- (7) Doolittle, A. K. *J. Appl. Phys.* 1952, 23, 418.
- (8) “International Critical Tables of Numerical Data, Physics, Chemistry and Technology”; McGraw-Hill, New York: Vol. 3, pp 27, 28; Vol. 5, p 26; Vol. 7, p 213.
- (9) Bohdanecký, M.; Kovář, J. “Viscosity of Polymer Solutions”; Elsevier Scientific: New York, 1982; pp 202, 208.
- (10) Berne, B. J.; Pecora, R., ref 5, pp 143–150.
- (11) Bauer, D. R.; Brauman, J. I.; Pecora, R. *Annu. Rev. Phys. Chem.* 1976, 27, 443.
- (12) McCall, D. W. *Acc. Chem. Res.* 1971, 4, 223.

## Normal-Coordinate Analysis of the Dynamics of Cubic Lattice Models of Polymer Chains

Michelle Dial, Katherine S. Crabb,<sup>†</sup> Charles C. Crabb,<sup>†</sup> and Jeffrey Kovac\*

Department of Chemistry, University of Tennessee, Knoxville, Tennessee 37996-1600.  
Received March 4, 1985

**ABSTRACT:** The dynamic behavior of isolated cubic lattice model polymer chains was simulated with and without excluded volume by using a Monte Carlo method. The chain relaxation was analyzed by using the Rouse normal coordinates. For the first three normal modes we find that the relaxation times conform fairly well to the prediction of the Rouse theory in the absence of excluded volume, but in the presence of excluded volume, there are deviations in both the  $N$  dependence and the  $k$  dependence of the relaxation times.

## Introduction

In a recent paper Gurler, Crabb, Dahlin, and Kovac<sup>1</sup> developed a model for the simulation of the dynamics of cubic lattice models of polymer chains using a Monte Carlo method. This model differed from most of the previous work<sup>2</sup> on the cubic lattice model in that one of the elementary motions employed was the 90° crankshaft. The dynamics of isolated chains were studied both in the presence and absence of excluded volume. Both the end-to-end vector relaxation time and the center-of-mass diffusion constant were computed, and the results were found to agree fairly well with the results of the Rouse model<sup>3</sup> in the absence of excluded volume and with the scaling prediction for chains with excluded volume.<sup>4</sup> The model has been extended to multiple chain systems by Crabb and Kovac<sup>5</sup> in order to investigate the effects of entanglements on chain dynamics.

The results of Gurler, Crabb, Dahlin, and Kovac raised several questions that prompted the more detailed study of the chain dynamics reported in this paper. The first question concerns the calculation of the end-to-end vector relaxation time,  $\tau_R$ . In the paper of Gurler, Crabb, Dahlin, and Kovac this quantity was estimated by first computing

the end-to-end vector autocorrelation function,  $\rho_R(t)$ , defined by

$$\rho_R(t) = \frac{\langle \vec{R}(t) \cdot \vec{R}(0) \rangle}{\langle R^2 \rangle} \quad (1)$$

where  $\langle \rangle$  denotes an equilibrium ensemble average. This average was computed as a time average. A least-squares line was then fit to the linear, long-time region of a semilog plot of  $\rho_R(t)$  vs.  $t$ . The negative of the relaxation time,  $\tau_R$ , is then the inverse of the slope of this line. There is an obvious problem with this calculation. A choice of the linear region to be fit must be made, and this choice is somewhat arbitrary. Gurler, Crabb, Dahlin, and Kovac took care not to introduce bias through the choice of the linear region, but questions concerning the accuracy of their relaxation times remain. A less controversial procedure would be to calculate the autocorrelation function of the first ( $k = 1$ ) normal coordinate and calculate the relaxation time from the slope of a semilog plot of that function vs. time. The normal coordinates,  $\vec{U}_k(t)$ , are defined by<sup>6</sup>

$$\vec{U}_k(t) = \sum_{j=1}^N \left( \frac{2 - \delta_{k0}}{N} \right)^{1/2} \cos[(j-1)\pi k/N] \vec{R}_j(t) \quad (2)$$

where  $\vec{R}_j$  is the position of the  $j$ th bead with respect to the origin. The autocorrelation function of the  $k$ th normal coordinate,  $\rho_k(t)$ , is given by

\* To whom correspondence should be addressed.

<sup>†</sup> Present address: Rohm and Haas Research Laboratories, Rohm and Haas Company, Bristol, PA 19007.

$$\rho_k(t) = \frac{\langle \vec{U}_k(t) \cdot \vec{U}_k(0) \rangle}{\langle U_k^2 \rangle} \quad (3)$$

Gurler, Crabb, Dahlin, and Kovac found that the dependence of the relaxation time on chain length,  $N$ , changed from an approximate  $N^2$  dependence in the absence of excluded volume to an approximate  $N^{2.2}$  dependence in the presence of excluded volume. It would be interesting to see whether this same chain-length dependence holds for the characteristic relaxation times of the higher order normal modes. It would also be interesting to see if the  $k^{-2}$  dependence of the relaxation time on mode number predicted by the Rouse theory is altered by the presence of excluded volume. These two questions assume that the normal-mode concept is still applicable in the presence of excluded volume. Since the only previous study of the relaxation of higher order normal coordinates<sup>7</sup> concluded that cubic lattice chains with excluded volume do not have true normal coordinates, it is important to check this assumption as well.

We have investigated these questions by studying the relaxation of the first three normal modes of the cubic lattice model developed by Gurler, Crabb, Dahlin, and Kovac. The relaxation is investigated by computing the normal-mode autocorrelation function defined in eq 3. To test the validity of the normal-mode concept we have also computed both the magnitude of the static mode-mode cross correlation  $C_{kk'}$ , defined as

$$C_{kk'} = \langle \vec{U}_k \cdot \vec{U}_{k'} \rangle \quad (4)$$

and the mode-mode cross-correlation function, given by

$$Q_{kk'}(t) = \frac{\langle \vec{U}_k(t) \cdot \vec{U}_{k'}(0) \rangle}{\langle \vec{U}_k \cdot \vec{U}_{k'} \rangle} \quad (5)$$

Our principal objective has been to investigate the nature of the deviation from the Rouse model brought about by the inclusion of excluded volume.

### Model

The model used in the simulations is identical with the model used by Gurler, Crabb, Dahlin, and Kovac. The reader is referred to that paper for a detailed description.<sup>1</sup> Briefly, the chain consists of  $N$  beads ( $N - 1$  bonds) on a cubic lattice. In the absence of excluded volume multiple occupancy of sites is allowed. In the presence of excluded volume each site may contain no more than one bead. In the movement algorithm a bead is first chosen at random. Depending on the local configuration surrounding a bead, one of the elementary motions is attempted. The end bead, normal bead, and  $90^\circ$  crankshaft motions are the three elementary motions employed. Each attempted move is called a bead cycle. The time unit used throughout is  $N$  bead cycles.

All simulation runs were begun from a fully equilibrated configuration. From time to time the coordinates of all the beads were sampled and those coordinates used to compute the normal coordinates according to eq 2. The sampling interval depends on the mode number of the autocorrelation functions to be computed. Because of the shorter relaxation time, points more closely spaced in time are needed to accurately compute the autocorrelation functions of the higher order normal modes. These normal coordinates were then used to compute the normal-mode autocorrelation functions  $\rho_k(t)$  by using eq 3, the static mode-mode cross correlations,  $C_{kk'}$ , by using eq 4, and the mode-mode cross-correlation functions,  $Q_{kk'}(t)$ , by using eq 5. In all cases the equilibrium ensemble averages were computed as time averages. The relaxation times  $\tau_k$  were calculated by fitting a least-squares line to a semilog plot

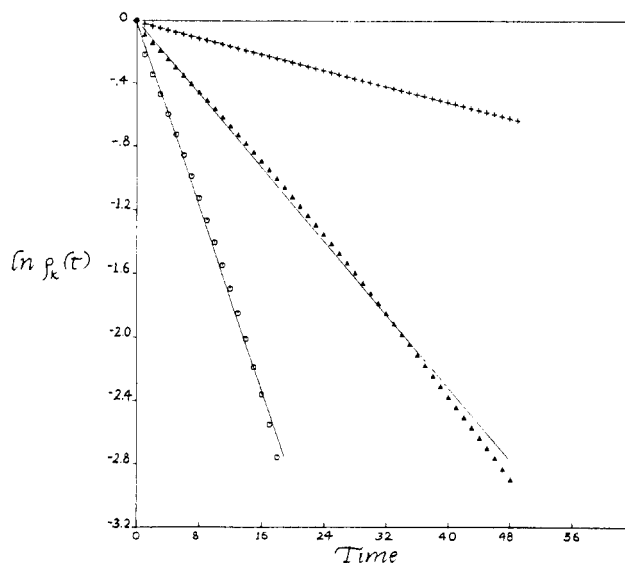


**Figure 1.** Semilogarithmic plots of the autocorrelation functions  $\rho_k(t)$  vs.  $t$  for the modes  $k = 1$  (+),  $k = 2$  (▲), and  $k = 3$  (○) for a chain of length  $N - 1 = 23$  in the absence of excluded volume. Also shown are the least-squares lines used to determine the relaxation times  $\tau_k$ .

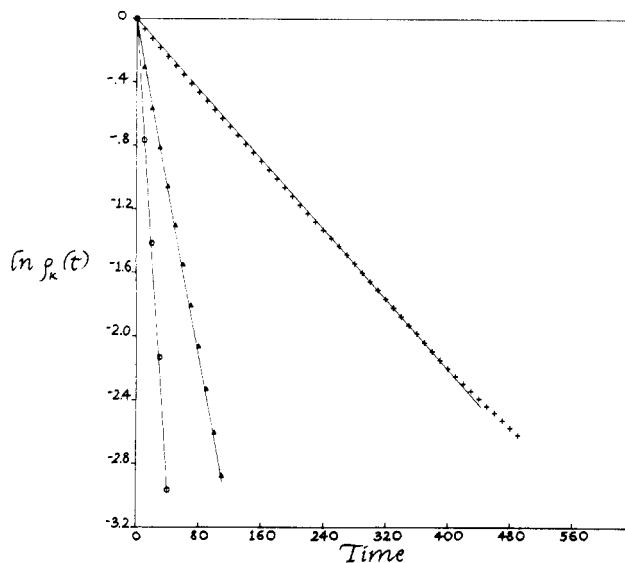


**Figure 2.** Semilogarithmic plots of the autocorrelation functions  $\rho_k(t)$  vs.  $t$  for the modes  $k = 1$  (+),  $k = 2$  (▲), and  $k = 3$  (○) for a chain of length  $N - 1 = 23$  in the presence of excluded volume. Also shown are the least-squares lines used to determine the relaxation times  $\tau_k$ .

of  $\rho_k(t)$  vs. time. The negative of the relaxation time is then the inverse of the slope of this line.

### Results and Discussion

Monte Carlo simulations were carried out for chains of lengths 11, 23, 35, 47, and 59 bonds, with and without excluded volume. At least six runs were done for each chain length and mode number. The autocorrelation functions obtained for the individual simulation runs were then averaged to reduce statistical errors.

The averaged semilogarithmic plots of the autocorrelation functions,  $\rho_k(t)$ , for  $k = 1, 2, 3$  are shown for chains of length  $N - 1 = 23$  in Figures 1 and 2 and for chains of length  $N - 1 = 59$  in Figures 3 and 4. Both the non-excluded-volume and the excluded-volume cases are shown.

These results are typical of those obtained for the other chain lengths. Also shown are the unweighted least-squares lines used to calculate the relaxation times,  $\tau_k$ . In

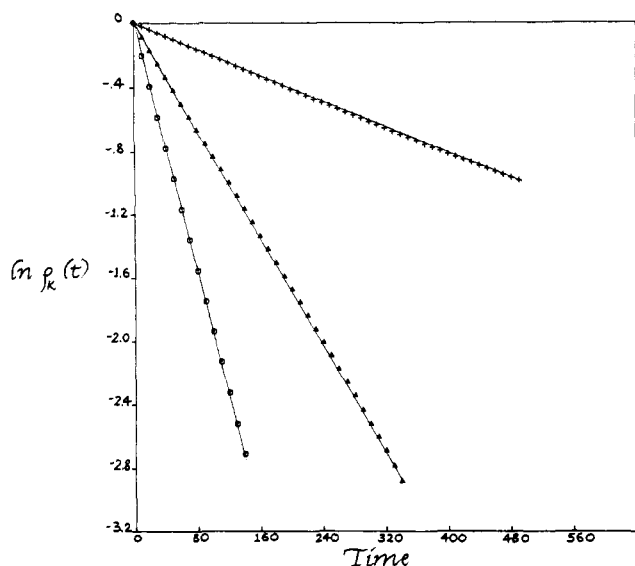


**Figure 3.** Semilogarithmic plots of the autocorrelation functions  $\rho_k(t)$  vs.  $t$  for the modes  $k = 1$  (+),  $k = 2$  (▲), and  $k = 3$  (○) for a chain of length  $N - 1 = 59$  in the absence of excluded volume. Also shown are the least-squares lines used to determine the relaxation times  $\tau_k$ .

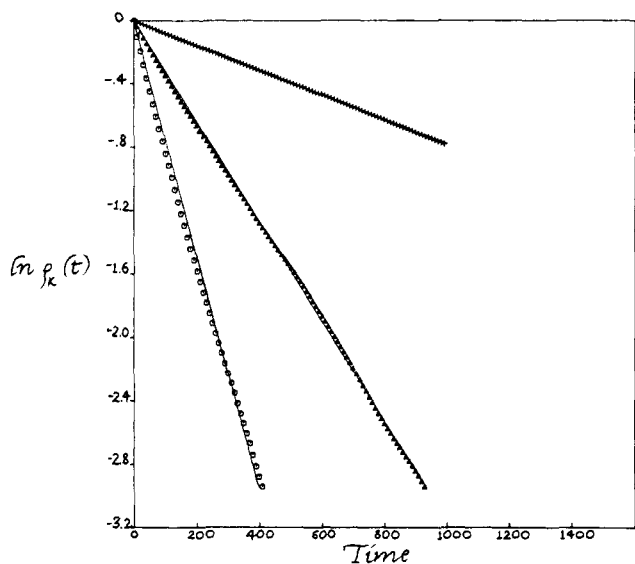


**Figure 4.** Semilogarithmic plots of the autocorrelation functions  $\rho_k(t)$  vs.  $t$  for the modes  $k = 1$  (+),  $k = 2$  (▲), and  $k = 3$  (○) for a chain of length  $N - 1 = 59$  in the presence of excluded volume. Also shown are the least-squares lines used to determine the relaxation times  $\tau_k$ .

all cases the least-squares line was fit over the interval  $0 \leq \ln \rho_k(t) \leq -1.2$ .

It is clear from Figures 1–4 that the decay of the autocorrelation functions  $\rho_k(t)$  is essentially exponential in both the absence and the presence of excluded volume. This strongly suggests that the Rouse coordinates defined in eq 2 are a good set of normal coordinates for cubic lattice chains even in the presence of excluded volume. In the only previous study of the relaxation of normal coordinates Verdier<sup>7</sup> found a strongly nonexponential decay of the normal modes in the presence of excluded volume. The model used by Verdier, however, differed considerably from the one used here. Verdier's simulation used only the normal-bead and end-bead movements. It has been suggested that the model used by Verdier in his normal-mode study introduces artificial constraints on the chain dynamics in the presence of excluded volume.<sup>8</sup> The non-exponential decay of the normal modes may be another

**Table I**  
Relaxation Times  $\tau_k$  as a Function of Chain Length ( $N - 1$ )

chain length, $N - 1$	relaxation times <sup>a</sup>			
	$\tau_1$	$\tau_2$	$\tau_3$	$\tau_R$ <sup>b</sup>
No Excluded Volume				
11	18.67	3.289	0.904	20.2
23	78.10	18.31	7.408	78.0
35	175.3	42.64	17.86	168.4
47	310.5	77.38	33.68	320.4
59	501.1	120.9	51.59	465.6
Excluded Volume				
11	36.49	6.574	1.264	38.5
23	180.97	38.14	13.04	179.3
35	425.0	101.2	38.00	441.3
47	809.3	187.0	78.48	874.5
59	1315.13	310.8	124.0	1326.2

<sup>a</sup> Time unit is  $N$  bead cycles. <sup>b</sup> Taken from ref 1.

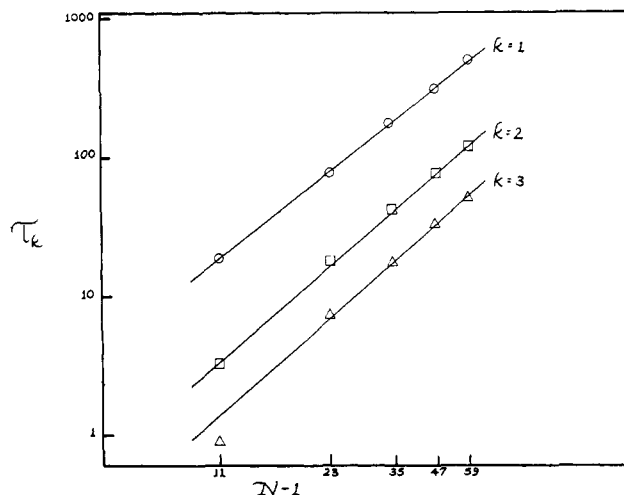


**Figure 5.** Scaling plot of  $\ln \tau_k$  vs.  $\ln(N - 1)$  at constant  $k$  in the absence of excluded volume. Also shown are the least-squares lines used to determine the scaling exponent  $\alpha_k$ .

manifestation of the effect of these constraints on the dynamics.

We have examined the question of the validity of the normal-mode concept in more detail by calculating the magnitudes of the static cross correlations  $C_{12}$  and  $C_{13}$  (cf. eq (4)). We find that in both the non-excluded-volume and the excluded-volume cases the values for  $C_{12}$  and  $C_{13}$  are statistically indistinguishable from zero and statistically indistinguishable from each other. Because of the extremely small values of the cross correlations, our attempts to calculate the mode-mode cross correlations  $Q_{kk'}(t)$  resulted mainly in statistical noise. In the few cases (mainly the longer chains) where the averaging process produced anything sensible we found that the cross correlation decayed to zero in a small fraction of the relaxation time of the faster mode. We therefore conclude that for the cubic lattice model the Rouse normal coordinates defined in eq 2 are a good set of normal coordinates even in the presence of excluded volume.

The values of the various relaxation times are collected in Table I. Also listed in Table I are the relaxation times,  $\tau_R$ , calculated by Gurler, Crabb, Dahlin, and Kovac using the long-time behavior of the autocorrelation function  $\rho_R(t)$ .<sup>1</sup> When the values for  $\tau_R$  and  $\tau_1$  are compared, it is clear that the long-time behavior of the autocorrelation function  $\rho_R(t)$  provides an accurate estimate of the relaxation time of the first normal mode of the chain. Table I confirms the accuracy of the results of Gurler, Crabb, Dahlin, and Kovac.

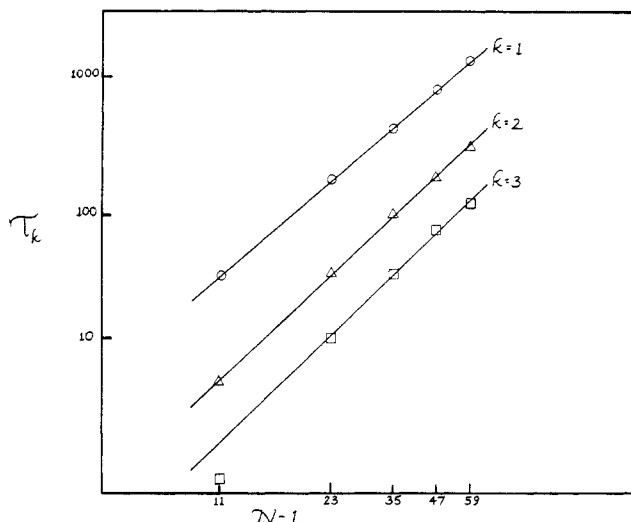


**Figure 6.** Scaling plot of  $\ln \tau_k$  vs.  $\ln(N-1)$  at constant  $k$  in the presence of excluded volume. Also shown are the least-squares lines used to determine the scaling exponents  $\alpha_k$ .

**Table II**  
Values of the Scaling Exponent  $\alpha_k$ , Defined in Equation 6 as a Function of Mode Number,  $k$

mode number, $k$	no excluded volume	excluded volume
1	1.95	2.13
2	2.14	2.30
3	2.07	2.41

To further analyze the relaxation behavior we have made scaling plots to extract both the  $N$  dependence and the  $k$  dependence of the relaxation times. Figures 5 and 6 are scaling plots of  $\ln \tau_k$  vs.  $\ln(N-1)$  at constant  $k$  for all three modes. Both the non-excluded-volume and excluded-volume cases are shown. Except for the  $k=3$  mode for  $N=12$  the points for each mode lie very close to a straight line. The data for each mode have been fit by using an unweighted least-squares line. These lines are also shown in the figures. The  $k=3$ ,  $N=12$  points have not been used in these fits. The slopes can be identified with scaling exponents through the relation

$$\tau_k \sim (N-1)^{\alpha_k} \quad (6)$$

The values for  $\alpha_k$  are collected in Table II.

To investigate the  $k$  dependence of the relaxation times we have made scaling plots of  $\ln \tau_k$  vs.  $\ln k$  at constant  $N$ . These are shown in Figures 7 and 8 for the non-excluded- and excluded-volume cases, respectively. Also shown are least-squares lines used to determine a scaling exponent for the relationship

$$\tau_k \sim k^{-\gamma_N} \quad (7)$$

The values for  $\gamma_N$ , which are the negatives of the slopes of the least-squares lines, are collected in Table III. The points for  $k=3$ ,  $N=12$  were again excluded from the analysis.

The points for  $k=3$ ,  $N=12$ , were not excluded merely because they did not fit the scaling relation neatly. A simple analysis shows that the results in this case cannot be compared to the other data. In any lattice model simulation it is important that the length scale of the motion being studied be much longer than the length scale of the elementary motions employed in the stimulation. Otherwise one is looking only at the elementary motions and not at their cooperative effects. The length scale of motions probed by the higher order normal modes is approximately  $N/k$  bonds. The length scale of the elemen-

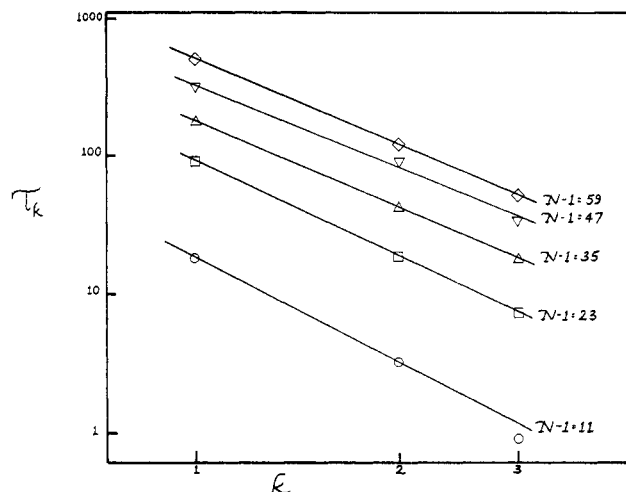


**Figure 7.** Scaling plot of  $\ln \tau_k$  vs.  $\ln k$  at constant  $N$  in the absence of excluded volume. Also shown are the least-squares lines used to determine the scaling exponents  $\gamma_N$ .

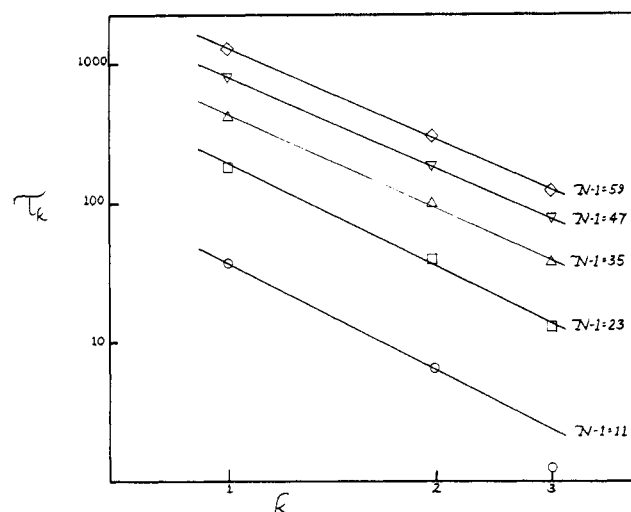


**Figure 8.** Scaling plot of  $\ln \tau_k$  vs.  $\ln k$  at constant  $N$  in the presence of excluded volume. Also shown are the least-squares lines used to determine the scaling exponents  $\gamma_N$ .

**Table III**  
Values of the Scaling Exponent  $\gamma_N$ , Defined in Equation 7 as a Function of the Chain Length  $N$

chain length, $N$	no excluded volume	excluded volume
12	2.50	2.47
24	2.13	2.38
36	2.07	2.18
48	2.02	2.12
60	2.07	2.14

tary motions in this model is three bonds. For the  $k=3$ ,  $N=12$  case these two lengths are essentially equal. For all other cases  $N/k$  is six, which is twice the length scale of the elementary motions. Therefore we felt quite justified in excluding the  $k=3$ ,  $N=12$  points in our analysis. Further evidence to justify this exclusion will be presented below.

Examination of Tables II and III reveals some interesting aspects of the chain dynamics. The exponent  $\alpha_k$ , which describes the  $N$  dependence of the relaxation times, is much closer to 2.0 in the non-excluded-volume case than in the excluded-volume case. The excluded-volume exponent is consistently larger than the non-excluded-volume value. The deviations from approximately Rouse-like behavior observed for the end-to-end vector relaxation persist in the higher order normal modes. If anything, the

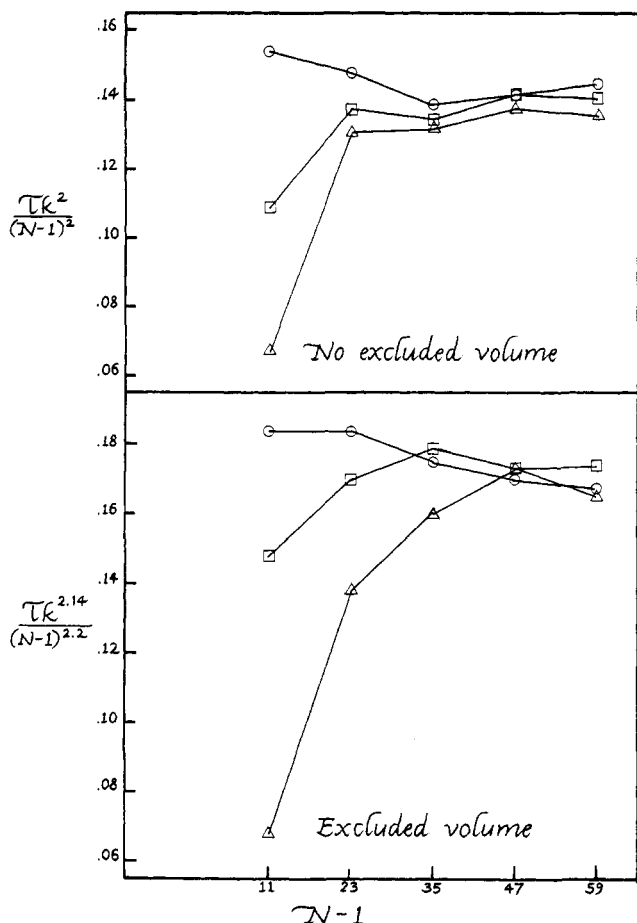


**Figure 9.** Plot of the quantity  $[\tau_k(N)k^2/(N-1)^2]$  in the absence of excluded volume and  $[\tau_k(N)k^{2.14}/(N-1)^{2.2}]$  in the presence of excluded volume as a function of the chain length  $(N-1)$ . Values are shown for all three modes:  $k=1$  (○),  $k=2$  (□),  $k=3$  (△). The lines are drawn only to guide the eye.

deviations are somewhat stronger for the  $k=2$  and  $k=3$  modes.

The exponent  $\gamma_N$  shown in Table III varies with increasing  $N$ . At  $N=12$   $\gamma_N$  is considerably larger than the Rouse value of 2.0 for both the non-excluded-volume and excluded-volume cases. These values are not very reliable since they are calculated from only two points, and it may well be that even the relaxation of the  $k=2$  mode for this chain is showing the local motion effects discussed above in the context of the  $k=3$  mode. The values for  $\gamma_N$  decrease with increasing  $N$ , seeming to level off for  $N=36, 48$ , and  $60$ . The values for the excluded-volume case are consistently a little higher than the values for non-excluded volume. This seems to indicate that in the excluded-volume case there is some deviation from the  $k^{-2}$  behavior predicted by the Rouse model.<sup>2</sup> The deviation is rather small and may be due either to statistical error or to the short chain lengths. We are inclined to view it as a real deviation since the value for  $\gamma_N$  in the excluded-volume case seems to be leveling off to a constant value larger than 2.0 as the chain length increases.

To explore the differences between the excluded-volume and non-excluded-volume cases a little further we have plotted the quantities  $[\tau_k(N)k^2/(N-1)^2]$  for the non-excluded-volume case and  $[\tau_k(N)k^{2.14}/(N-1)^{2.2}]$  in the excluded-volume case as a function of both  $k$  and  $(N-1)$  in Figures 9 and 10. The exponent for  $(N-1)$  in the excluded-volume case is the value predicted by scaling theory. The exponent for  $k$  in the excluded-volume case is the long-chain value obtained in our simulations. Figures 9 and 10 show that, except for the  $N=12$  chain, the

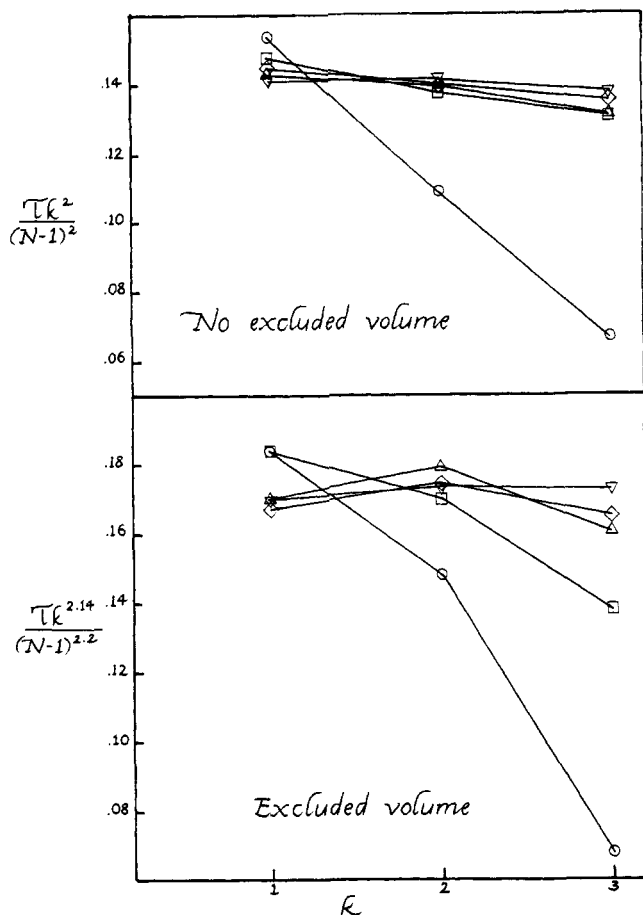


**Figure 10.** Plot of the quantity  $[\tau_k(N)k^2/(N-1)^2]$  in the absence of excluded volume and  $[\tau_k(N)k^{2.14}/(N-1)^{2.2}]$  in the presence of excluded volume as a function of the mode number  $k$ . Values are shown for all chain lengths:  $N-1=11$  (○),  $N-1=23$  (□),  $N-1=35$  (△),  $N-1=47$  (▽),  $N-1=59$  (◇). The lines are drawn only to guide the eye.

dynamics of the cubic lattice model conform quite well to the Rouse prediction in the absence of excluded volume. A little more scatter is observed in the presence of excluded volume, but the data are fairly well fit by the exponents chosen, particularly at the longer chain lengths. A comparison of Figures 9 and 10 strongly suggests that in the presence of excluded volume there is a deviation from Rouse-like behavior in both the  $N$  dependence and the  $k$  dependence of the relaxation times. The  $k$  dependence of the relaxation times in the presence of excluded volume clearly deserves further study.

### Conclusion

The normal-mode analysis of the chain dynamics has revealed several interesting things. For chains without excluded volume approximately Rouse-like behavior in both  $N$  and  $k$  is seen in the higher normal modes, as long as the length scale of the mode being studied is much longer than the length scale of the elementary motions. The presence of excluded volume causes deviations from Rouse-like behavior in the  $N$  dependence of the relaxation times even in the higher normal modes. A deviation in the  $k$  dependence of the relaxation times also occurs. A study of the mode-mode cross correlations indicates that the Rouse normal coordinates are a good set of normal coordinates for the cubic lattice model even in the presence of excluded volume.

**Acknowledgment.** Acknowledgment is made to the Department of Energy, Division of Materials Sciences, Office of Basic Energy Sciences, for partial support of this

research. Acknowledgment is also made to the donors of the Petroleum Research Fund, administered by the American Chemical Society, for partial support of this research. We also thank the University of Tennessee Computer Center for their continuing support and patience.

## References and Notes

- (1) Gurler, M. T.; Crabb, C. C.; Dahlin, D. M.; Kovac, J. *Macromolecules* 1983, 16, 398.
- (2) Kranbuehl, D. E.; Verdier, P. H. *J. Chem. Phys.* 1979, 71, 2662 and references therein.
- (3) Rouse, P. E. *J. Chem. Phys.* 1953, 21, 1273.
- (4) de Gennes, P. G. "Scaling Concepts in Polymer Physics"; Cornell University Press: Ithaca, NY, 1979.
- (5) Crabb, C. C.; Kovac, J. *Macromolecules* 1985, 18, 1430.
- (6) Verdier, P. H. *J. Chem. Phys.* 1966, 45, 2118.
- (7) Verdier, P. H. *J. Chem. Phys.* 1973, 59, 6119.
- (8) Hilhorst, H. J.; Deutch, J. M. *J. Chem. Phys.* 1975, 63, 5153.

# Steady-State Compliance of Linear Polymer Solutions over a Wide Range of Concentration

Yoshiaki Takahashi,\* Ichiro Noda, and Mitsuru Nagasawa

Department of Synthetic Chemistry, Nagoya University, Furo-cho, Chikusa-ku, Nagoya 464, Japan. Received February 13, 1985

**ABSTRACT:** Measurements of zero-shear viscosity  $\eta^\circ$  and steady-state compliance  $J_e$  of linear polystyrenes with high molecular weights were carried out in good and poor solvents with a Weissenberg rheogoniometer to examine the applicability of the scaling theory of de Gennes to  $J_e$ . It was confirmed, in agreement with a previous work, that the experimental data of  $\eta^\circ$  in semidilute solutions agree with predictions of the scaling theory. However, the scaling theory did not agree with the experimental data of  $J_e$ . It was concluded that the idea of a semidilute region need not be brought in to understand  $J_e$  of linear polymer solutions.

## Introduction

Theories of the molecular weight ( $M$ ) and polymer concentration ( $C$ ) dependences of the zero-shear viscosity  $\eta^\circ$  of linear polymers<sup>2,3</sup> as well as of their osmotic pressure  $\Pi$ <sup>4</sup> are based on quite different models in dilute and concentrated solutions. It was reported<sup>1,5-7</sup> that the gap between the theories for dilute and concentrated solutions can be filled if we recognize the existence of so-called semidilute solutions as proposed by de Gennes.<sup>8</sup> In the semidilute region it is assumed that the polymer coils overlap each other but the segment density is still so low that the excluded volume effect works between segments. Also, the polymer concentration dependence of a property in semidilute solution can be predicted by the scaling method of de Gennes.<sup>8</sup>

That is, if we define a viscosity parameter  $\eta_R^\circ$  by

$$\eta_R^\circ \equiv \eta_{sp}^\circ / C[\eta]$$

where  $\eta_{sp}^\circ = (\eta^\circ - \eta_s)$ ,  $\eta_s$  is the solvent viscosity, and  $[\eta]$  is the intrinsic viscosity,  $\eta_R^\circ$  of semidilute solutions is given by<sup>1</sup>

$$\eta_R^\circ \propto (C/C^*)^{(4.4-3\nu)/(3\nu-1)} \quad (1)$$

or

$$\eta_{sp}^\circ \propto M^{3.4} C^{3.4/(3\nu-1)} \quad (2)$$

where  $C^* = 3M/(4\pi\langle S^2 \rangle^{3/2} N_A)$  is the critical concentration at which polymer coils begin to overlap each other and  $\nu$  is an excluded volume exponent defined as  $\langle S^2 \rangle \propto M^{2\nu}$ .  $\langle S^2 \rangle$  is the mean square radius of gyration and  $N_A$  is Avogadro's number. In dilute solutions,  $\eta_R^\circ$  is given by

$$\eta_R^\circ = 1 + k(C/C^*) + \dots \quad (3)$$

where  $k = 3km\Phi/4\pi N_A$  and  $k'$  and  $\Phi$  are the Huggins constant and the Flory coefficient, respectively. It was reported in a previous paper<sup>1</sup> that the predictions of eq 1-3 are in agreement with the experimental data of poly( $\alpha$ -methylstyrenes) (P $\alpha$ MS) in good solvents as well as in

$\Theta$  solvents if the molecular weights of the polymers are sufficiently high.

The viscoelastic properties of polymer solutions of melts, however, can be described by two parameters expressing the energy dissipation and storage mechanisms, such as zero-shear viscosity  $\eta^\circ$  and steady-state compliance  $J_e$ . The purpose of this work is to examine whether or not the concept of the semidilute region is useful for understanding not only  $\eta^\circ$  but also  $J_e$  over the entire range of polymer concentrations. The molecular weight and polymer concentration dependences of the steady-state compliance  $J_e$  of linear polymers are also different in different regions.<sup>2,3</sup> If the polymer concentration is below a certain value,  $J_e$  becomes proportional to  $M/C$ , in agreement with the modified Rouse theory for the viscoelastic properties of unentangled polymers. We call this region the Rouse region in this paper, though the original Rouse theory should be applied to infinitely dilute solution. If we define  $J_{eR}$  by

$$J_{eR} \equiv [J_e CRT/M][\eta^\circ/(\eta^\circ - \eta_s)^2]$$

$J_{eR}$  is a constant independent of molecular weight and polymer concentration in the Rouse region. The constant is  $\sim 0.4$  in good solvents and higher in poor solvents. In concentrated solutions or in melts, on the other hand, the polymer molecules are extensively entangled with each other so that all entanglement points are distributed uniformly in the solution. Then the entanglement density is proportional to  $C^2$ , and  $J_e$  should be proportional to  $C^{-2}$  independent of  $M$  and the solvent if the conformation of the polymer chain between two adjacent entanglement points is Gaussian. That is

$$J_e \propto C^{-2} \quad (4)$$

or

$$J_{eR} \propto (CM)^{-1} \quad (5)$$

The region is often called the network region. These speculations were found to agree with experimental data